Bounds for BEM Capacitance Extraction*

Michael W. Beattie and Lawrence T. Pileggi
Carnegie Mellon University
Department of Electrical and Computer Engineering
Pittsburgh, PA 15213

Abstract

In this paper we prove that simply discarding conductors beyond a certain spacing during BEM capacitance extraction will result in a lower bound on the self-capacitance calculations and an upper bound on the mutual capacitance calculations that lie within that spacing. We prove that a potential-shift and truncate scheme can yield bounds opposite to those for the truncate only case; namely, an upper bound on the self capacitance and a lower bound on the mutual capacitance that lies within the chosen spacing. The ease with which the upper and lower bounds are calculated is shown, and their utility for selection of an optimal window size is described. A metal shell is also presented here that results in bounds similar to those of shift–truncate. We further propose a new potential–shift function that yields increased approximation accuracy compared to shift–truncate in many cases.

1 Introduction

Boundary element methods (BEM) have been used extensively for parasitic capacitance extraction [3][6]. Several different techniques for the *localization* of the extracted capacitance have been developed, such as scanning methods [4][7] which build capacitance databases of the elementary conductor constellations encountered in the circuit, and windowing techniques.

This paper proves that the *shift–truncate method* from [1] and the *windowing method* yield opposite bounds for the exact values of the mutual and self capacitances. We also introduce the *metal shell* [2] featuring the same bounds as shift–truncate and the *homogenously filled shell* which provides a higher accuracy than shift–truncate [2] in many cases. Furthermore, we propose a methodology that will use these bounds to determine the optimal size of the window.

2 Bounds for C Extraction with BEM

In this section we will show that the *windowing method* yields lower bounds for the two–terminal self capacitances and upper bounds for the two–terminal mutual capacitances, and that the corresponding bounds for the *shift–truncation technique* [1] are the opposite. Background information about BEM and the terminology used here can be found in section 2 of [1].

2.1 Bounds of the Windowing Technique

In Fig. 1 the reference conductor is the shaded one. Mutual capacitances are calculated with respect to this conductor. All conductors outside of the window are ignored in the subsequent calculation of the capacitances, leading to a significantly smaller potential matrix to be inverted.

With windowing, $C_{i,jx1}$ may be different from $C_{jx1,i}$, since i has a different set of conductors in its window than those in the window for the j_{x1} conductor. This renders the complete C matrix (for the entire system) asymmetric. In such cases, and since they are bounds (as we will show below), one may choose the smaller two–terminal mutual and the larger two–terminal self capacitance, to be nearer to the exact values.

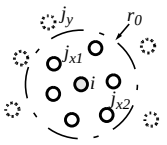

Fig. 1 Windowing

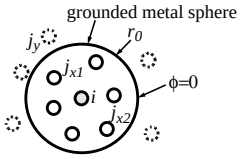

Fig. 2 Metal Shell

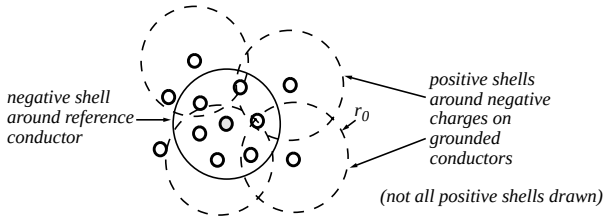

Fig. 3 Shift–truncation method

Let i be the index of the reference conductor, $\{j_x\}$ the set of indices of all other conductors *inside* the window of i, and $\{j_y\}$ the set of indices of all other conductors *outside* of the window of i. It is known, if i is assigned a unit potential and all other conductors are grounded, then the charge on i will be the (short circuit) self capacitance C_{ii} of i, and the q_j's are the mutual (short circuit) capacitances C_{ij} [8]. The linear system describing this problem is

$$P\hat{q} = \hat{e}_i = \begin{bmatrix} 0 \\ \vdots \\ 0 \\ 1 \\ 0 \\ \vdots \\ 0 \end{bmatrix} \leftarrow \text{i}^{\text{th}} \text{ element} \qquad (1)$$

where

$$P = \begin{bmatrix} [P_s] & [P_{sy}] \\ [P_{sy}]^T & [P_y] \end{bmatrix} \qquad (2)$$

P is the potential matrix of the entire system, P_s that of the system in the window, and P_y that of the system of all conductors outside of the present window. Therefore, all three of these matrices are symmetric and positive definite, as well as diagonally dominant. P_{sy} is

* This work was supported in part by the Semiconductor Research Corporation under contract DC-068.

DAC 1997, Anaheim, California

the matrix which couples the conductors inside the window with those outside.

After introducing the window, the charge on the conductors $\{j_y\}$ are forced to zero, so their potential is *not fixed* anymore. Fixing the potential on the conductors $\{j_y\}$ which are outside of the window, in addition to fixing the charges to zero, would lead to an overdetermined linear system, which might not have a solution. The rows of (1) corresponding to the potentials on the outside conductors are now no longer necessary, so that the lower row of (2) falls away. Since the charges on the conductors $\{j_y\}$ are zero in the altered system, (1) can now be written as

$$P_s \begin{bmatrix} \underset{\sim}{q}_i \\ \underset{\sim}{q}_{\{jx\}} \end{bmatrix} = \hat{e}_i = \begin{bmatrix} [P_s] & [P_{sy}] \end{bmatrix} \begin{bmatrix} q_i \\ q_{\{jx\}} \\ q_{\{jy\}} \end{bmatrix} \tag{3}$$

where $\underset{\sim}{q}$ represents the charges on the conductors in the altered system (after forcing the charge on the outside conductors to zero) and q specifies the charges in the original, exact system. The indices are defined as above with reference to Fig. 1. From the above we know, that $\underset{\sim}{q}_{\{jy\}} = \hat{0}$. Defining

$$\Delta q_k = \underset{\sim}{q}_k - q_k \quad ; \quad k \in \{i, \{j_x\}, \{j_y\}\} \tag{4}$$

as the charge change on the conductors after introducing the window, eq. (3) can be written as

$$P_s \begin{bmatrix} \Delta q_i \\ \Delta q_{\{jx\}} \end{bmatrix} = P_{sy} q_{\{jy\}} = \sum_{k \in \{jy\}} \left(P_{sy}\big|_{column\ k} \cdot q_k \right) \tag{5}$$

The sum on the right side represents the superposition of the potentials caused on the surfaces of i and $\{j_x\}$ by the charges $q_{\{jy\}}$. Equation (5) can be also written as

$$P_s \begin{bmatrix} \Delta q_i \\ \Delta q_{\{jx\}} \end{bmatrix} + \sum_{k \in \{jy\}} \left(P_{sy}\big|_{column\ k} \cdot (-q_k) \right) = \hat{0} \tag{6}$$

The linear system described in (6) represents a set of conductors $\{i, \{j_x\}\}$ which are connected to ground (right side is identical zero), while the conductors $\{j_y\}$ carry charges *opposite* to those they had in the original system. Now we look at the similar systems:

$$P_s \begin{bmatrix} \Delta q_i^{(k)} \\ \Delta q_{\{jx\}}^{(k)} \end{bmatrix} + P_{sy}\big|_{column\ k} \cdot (-q_k) = \hat{0} \quad ; \quad \forall k \in \{j_y\} \tag{7}$$

Equation (7) is the same as (6), except that in each of the rows in (7) only *one* of the conductors from $\{j_y\}$ carries the opposite of its normal charge, while all other conductors from $\{j_y\}$ do not exist. Since this is a system with several *grounded* conductors and one charged conductor, and it is known that q_k is negative $\forall k \in \{j_y\}$, we can conclude, that the elements of $\Delta q_{i\&\{jx\}}^{(k)}$ are *negative or zero* for all k. Superposing all systems represented by the equations in (7), we get back to (6), and can conclude, that the charge changes on the conductors inside the window due to ignoring the outside conductors are always *less or equal zero*.

Since this property is independent of the choice of the reference conductor, *all* of the elements of the *short circuit* capacitance matrix are less or equal their exact values. Therefore — due to their definitions [8] — the *two terminal* self capacitance is underestimated while the two terminal mutual capacitances — between conductors in the window only — are overestimated.

2.2 Bounds for Shift–Truncate

In many cases, bounds opposite to those gained with the windowing technique are desired, largely to obtain a pessimistic approximation of the self capacitance. As we will show, the *shift–truncate potential method* proposed in [1] and depicted in Fig. 3 yields such bounds.

Referring to Fig. 3, the reference conductor is again the shaded conductor. With the shift–truncate approach, instead of a window, each charge on the conductors is assumed to posess an oppositely charged shell of radius r_0 so that the charge *does not* interact with other charges further away than r_0. Assuming all of the conductors are small (panels of BEM), their shells are also approximately spherical. The shell of the reference conductor is negative (solid), all other shells are positive (dashed). *None* of the conductors is ignored, but all potential matrix entries between conductors farther away than r_0 are zero, making their charges zero as in windowing. But unlike windowing, thereby all outside conductor charges are *naturally* (continuous potential function at $r=r_0$) zeroed by the potential function. Thus there is no "window" *per se*. For this reason it is imperative that the shift–truncate scheme must produce a positive definite potential matrix. This can be assured by using shells that are physically based [1].

The boundary conditions (unit potential on the reference conductor i and all $\{j_x\}$ and $\{j_y\}$ conductors connected to ground) are the same for the *exact system* $(P;q)$ and the *shift–truncate system* $(\underset{\sim}{P};\underset{\sim}{q})$:

$$\underset{\sim}{P}\underset{\sim}{q} = Pq = \hat{e}_i \tag{8}$$

Using (4) and the definition

$$P_{sh} = \underset{\sim}{P} - P \tag{9}$$

(8) can be transformed into

$$\underset{\sim}{P}\Delta q = -P_{sh} q \tag{10}$$

Since $\underset{\sim}{P}$ is positive definite [1], $det[\underset{\sim}{P}] > 0$ and the solution Δq of (10) exists and is unique. Equation (10) can be also written as

$$P\Delta q = -P_{sh} q - P_{sh} \Delta q \tag{11}$$

and its solution must exist and be unique (equivalence with (10)). To consider the effect of the introduction of the shells in an incremental fashion, we create an iterative representation of Δq by using the recursive definition

$$P\Delta q^{(0)} = -P_{sh} q \tag{12}$$

$$P\Delta q^{(\nu)} = -P_{sh} \Delta q^{(\nu-1)} \quad ; \quad \forall \nu \in \{1;2;3;\ldots\} \tag{13}$$

Equation (13) properly defines all $\Delta q^{(\nu)}$. Since P is positive definite, the solutions of all equations in (12) and (13) exist and are unique.

Summing over all of the equations in (12), (13) and exploiting the linearity of P and P_{sh} yields

$$P \sum_{\nu=0}^{\infty} \Delta q^{(\nu)} = -P_{sh} q - P_{sh} \sum_{\nu=0}^{\infty} \Delta q^{(\nu)} \tag{14}$$

where (11) and (14) are similar linear systems. Therefore, $\sum_{\nu=0}^{\infty} \Delta q^{(\nu)}$ converges (existence) and

$$\sum_{\nu=0}^{\infty} \Delta\dot{q}^{(\nu)} \equiv \Delta\dot{q} \qquad \text{(uniqueness)} \tag{15}$$

Now it is known that in the exact system the total amount of charge must be positive [8]:

$$\sum_{k=1}^{N} q_k > 0 \quad with \quad q_i > 0 \quad and \quad q_{j\neq i} \leq 0 \tag{16}$$

where *i* is the reference conductor. Using (16) we will show in the following paragraphs that $-P_{sh}\dot{q}$ is a *non–negative* vector, thereby indicating that (12) describes the system of conductors with a negative background potential.

If $r_{ik} \leq r_0$, then $(-P_{sh}\dot{q})_k$ — with *k* being the index of a conductor satisfying this condition — is, due to the definitions of P, $\underset{\sim}{P}$ *and* P_{sh}, equal to

$$\frac{q_i}{4\pi\varepsilon r_0} + \sum_{j\neq i} \frac{q_j}{4\pi\varepsilon r} \quad with \quad r = \left\{ \begin{array}{ll} r_0 & if \ r_{kj} \leq r_0 \\ r_{kj} & if \ r_{kj} > r_0 \end{array} \right\} \geq r_0 \tag{17}$$

Here is $r_{ll} > 0$, but of the order of the size of a boundary element, so that we still can consider the conductors to be pointlike. Here we are making the assumption that the BEM is *exact*.

Since all $q_{j\neq i}$ are negative or zero from (16), the sum in (17) becomes *smaller* when we replace *r* under the sum with r_0. Factoring $1/4\pi\varepsilon r_0$ out of the new sum, using (16) and the fact that we have underestimated the exact expression, leads to

$$(-P_{sh}\dot{q})_k \geq 0 \quad for \ r_{ik} \leq r_0 \tag{18}$$

For $r_{ik} > r_0$ the elements $(-P_{sh}\dot{q})_k$ are equal to

$$\frac{q_i}{4\pi\varepsilon r_{ki}} + \sum_{j\neq i} \frac{q_j}{4\pi\varepsilon r} \quad with \quad r = \left\{ \begin{array}{ll} r_0 & if \ r_{kj} \leq r_0 \\ r_{kj} & if \ r_{kj} > r_0 \end{array} \right\} \geq r_0 \tag{19}$$

Replacing *r* in the sum with r_{kj} decreases its value, since all $q_{j\neq i}$ are negative or zero (16) and $r_{kj} \leq r$ by definition. The underestimated sum is

$$\sum_{l=1}^{N} \frac{q_l}{4\pi\varepsilon r_{kl}} \tag{20}$$

This expression is known to be zero, since *k* can only be a grounded conductor ($r_{ik} > r_0$), and (20) is *exactly* the potential on the surface of *k*. Since (20) underestimates the value of $(-P_{sh}\dot{q})_k$, we can conclude that $(-P_{sh}\dot{q})_k \geq 0$ for $r_{ik} > r_0$. Together with (18) it follows that the potential vector $(-P_{sh}\dot{q})$ — which is the right hand side of (12) — is *non–negative*.

We point out that in the previous paragraphs the restriction of the potential function to that of the shift–truncate shell was necessary to show the non–negativity of $(-P_{sh}\dot{q})$. Therefore this proof cannot be extended to the new shell potentials which will be investigated in section 3.

Equation (12) can be interpreted as describing a system of conductors with *all* conductors grounded while a *non–positive* background potential — caused by shell charges $P_{sh}\dot{q}$ — is present. If the background potential were zero, the charge on the grounded conductors would be trivially zero. Adding the background potential caused by the shell charges *while leaving the charge on the conductors unchanged* will cause the surface potential of the conductors to become negative. To re–establish the ground potential on the surfaces of the conductors, one must connect them to *positive* voltage sources. This is equivalent to adding positive charges to the surface of the conductors. $\Delta\dot{q}^{(0)}$ — the solution of (12) — is therefore also *non–negative*:

$$\Delta\dot{q}^{(0)} \geq \dot{0} \tag{21}$$

Now assume that $\Delta\dot{q}^{(\nu-1)}$ were known to be non–negative. Equation (13) determines the charges $\Delta\dot{q}^{(\nu)}$ which have to be on the surfaces of the conductors when all of the conductors are *grounded* and each conductor *k* is surrounded by a shell with radius r_0 and containing charge $-\Delta q_k^{(\nu-1)}$ (uniformly distributed). Since $\Delta\dot{q}^{(\nu-1)}$ is non–negative, *only negative charges* are causing the negative background potential. Because a negative point charge in a system of grounded conductors causes only positive or zero charge on each conductor (negative background potential) and the shells may be viewed as a superposition of negative point charges, the total charge on *each* conductor must be positive or zero. $\Delta\dot{q}^{(\nu)}$ is *non–negative*. With (21) and induction, it follows that this is the case for all $\nu \in \{0;1;2;\ldots\}$.

With (15) it can be finally shown, that $\Delta\dot{q}$ is *non–negative*. This is independent of the choice of the reference conductor; thus *all* of the elements of the *short circuit* capacitance matrix are greater than or equal to their exact values. The two–terminal self capacitance is therefore *overestimated* and the two–terminal mutual capacitances are *underestimated* using a shift–truncate scheme.

2.3 Metal shell method

A grounded metal sphere with a radius of r_0 and centered in the center of the reference conductor is added to the original system (see Fig. 1). This method yields bounds similar to those of the shift–truncate method. The proof [2] does not require the conductors to be pointlike as shift–truncate does. The metal shell method will therefore yield bounds even in cases for which the BEM has not converged sufficiently yet. Since the shell potential near the reference conductor is more negative on average in this case than for the shift–truncate method, the accuracy of the metal shell method will not be as high.

3 Physically Realizable New Shell Potentials

Numerical results show that the shift–truncate method results in upper bounds for the self capacitance (see Fig. 5) and lower bounds for the mutual capacitance, as predicted in section 2. The accuracy of the mutual capacitances, however, is low at times. Referring to Fig. 4, the reason for this behaviour becomes clearer. The potential

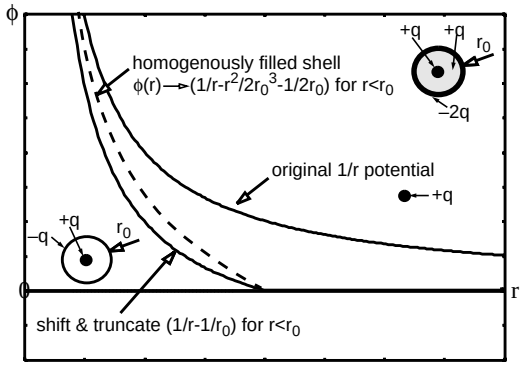

Fig. 4 Potential ϕ(r) of a point charge for different shells

created by a unit valued point charge is *lower* for all $r > 0$ (*including* $r < r_0$) for the shift–truncate case compared with the exact case. Shift–truncate *throws away* some of the capability of the electrical charges to create electrical potential. This is, of course, desirable for the region *outside* of r_0, but obviously the region within r_0 is also affected. This effect increases with the seperation distance between the grounded conductor and the reference conductor (within the "window").

To improve the accuracy it is desirable to *decrease the potential thrown away* by moving the potential curve nearer to the exact r^{-1} curve within r_0, while keeping the potential function continuous at r_0 and zero outside of r_0 to prevent the energy content of the shell charge distribution to be comparable to that of the original surface charge, which could lead to unstable capacitance matrices. The *homogenously filled shell* potential shown in Fig. 4 has the potential function $(1/r\text{-}r^2/2r_0^3\text{-}1/2r_0)$ for $r<r_0$ and has the desired properties.

It is important to use *physically realizable* shells to ensure the positive definiteness of the entire resulting capacitance matrix [1]. The appropriate charge distributions for the considered potential functions are also depicted in Fig. 4. If only the bounding properties are desired — as in the scheme described in section 4— methods such as the windowing technique, which does not generally yield positive definite matrices, may be used.

4 Selecting r_0 — Window size

We will see in section 5 that solving for both the windowing and shift–truncate case is quite straightforward. Given a limit for the error of the self and mutual capacitances, one may start calculating the short circuit capacitance matrix with a *small* value for r_0. In this case, windowing and the shell potential methods will be very efficient, since only a few elements of the potential matrix will remain nonzero. If the accuracy is not sufficient, r_0 may be increased gradually to include more distant conductors. To find a new value for r_0, we can exploit the fact that the shift–truncate capacitance values vary *continuously* with r_0 and estimate their derivatives at the current r_0. A modified version of the Newton–Raphson root–finding algorithm is then applied to determine the optimal r_0. The desired accuracy is reached when the differences of the upper and lower bounds for the self and mutual capacitances fall below a given threshold. That $r_{0,final}$ represents the distance above which the capacitive influence between conductors is negligible. A design flaw preventing the capacitive effects to remain localized is indicated by the resulting $r_{0,final}$ being too large after this procedure or exceeding a predefined maximum. This method may therefore generate design rules for limiting capacitance.

5 Results of Numerical Computations

To visualize the bounds for the shift–truncate method and to test the homogenously filled shell function, the capacitances of several simple but frequently appearing structures were calculated for a) different values of r_0, b) different shell types and c) different panelsizes (different accuracy of the BEM).

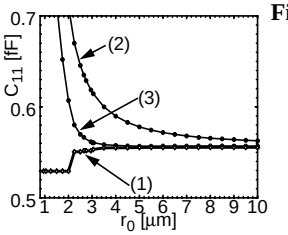

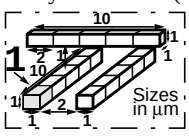

Fig. 5 Self capacitance error δC_{11} for system below calculated with windowing (1), shift–truncate (2), homogenously filled shell (3)

We used a zeroth order Galerkin–type BEM and the conjugate gradient squared method for the matrix inversion. During the calculation of the double integrals for the Galerkin–type potential matrix, the original Green's function $1/4\pi\varepsilon r$ is replaced by the alternative version for the particular shell potential. These are given in Fig. 4 (without the constant factor $1/4\pi\varepsilon$) for the shells used here. Since the Green's function can be implemented as a seperate function, which is called whenever the potential of a point charge is needed, changing the potential function only demands changing the formula in this one function and is therefore very easy to do. The accuracy of the self capacitance calculation is increased by using analytical formulas for the potential of specific boundary element forms (rectangular, triangle) derived with *Mathematica*.

For the windowing technique the original r^{-1} potential function is used but all panels which are further away than r_0 from the reference conductor are *deleted* from the set of conductors for the time of the calculation of this row of the capacitance matrix. This results in a small, dense matrix which must be inverted instead of a large sparse one.

The value of the shell potential function at *r=0 without the* r^{-1} *contribution* of the original point charge is crucial for the bounding properties, since decreasing the ability of the charges on the reference conductor to create potential increases the amount of charges necessary to keep the reference conductor at unit potential. The shift–truncate shell potential value at the origin is $-1/4\pi\varepsilon r_0$, which is provably negative enough.

6 Conclusion

It has been shown that the results of shift–truncation and windowing combined bound the exact capacitance values of a given conductor system. This can be exploited to automatically determine the appropriate window radius r_0 for this particular system.

In addition to this, further investigation of various — possibly anisotropic — potential functions and their properties with respect to sparsification for capacitance extraction is necessary.

Results from using shell potentials can be used as preconditioners for fast multipole method based capacitance extraction programs [5]. Integration of fast multipole methods into the calculation of the shell potentials could help further reducing the time necessary for calculating and inverting the potential matrix.

References

[1] B. Krauter, Y. Xia, A. Dengi, L. Pileggi, "A Sparse Image Method for BEM Capacitance Extraction", *33th Design Automation Conference Proceedings*, pp. 357–362, 1996.

[2] M. Beattie, M.S. Thesis, Carnegie Mellon University (Pittsburgh, USA), May 1997.

[3] N. P. van der Meijs, A. J. van Genderen, "An Efficient Finite Element Method for Submicron IC Capacitance Extraction", *26th ACM/IEEE Design Automation Conference Proceedings*, pp. 678–681, 1989.

[4] N. P. van der Meijs, "Accurate and Efficient Layout Extraction", Doctoral dissertation, Technische Universiteit Delft (Netherlands), 1992.

[5] K. Nabors, J. White, "FastCap: A Multipole Accelerated 3–D Capacitance Extraction Program", *IEEE Transactions on Computer-Aided Design*. vol. 10, No. 11, November 1991.

[6] C. Wei, R. F. Harrington, J. Mautz, T. Sarkar, "Multiconductor Transmission Lines in Multilayered Dielectric Media", *IEEE Transactions on Microwave Theory and Techniques*, vol. 32, No. 4, April 1984.

[7] N. Arora, K. Raol, R. Schumann, L. Richardson, "Modeling and Extraction of Interconnect Capacitances for Multilayer VLSI Circuits", *IEEE Transactions on Computer-Aided Design*. vol. 15, No. 1, January 1996.

[8] D. Ling, A. Ruehli, "Interconnection Modeling", in: *Circuit Analysis, Simulation and Design — Advances in CAD for VLSI Vol. 3, Part II* (Chapter 11), Elsevier Science Publishers B.V. (North–Holland), 1987.